A review of the electronic and magnetic properties of tetrahedrally bonded half-metallic ferromagnets



2007 J. Phys.: Condens. Matter 19 315221

(http://iopscience.iop.org/0953-8984/19/31/315221)

IOP PUBLISHING JOURNAL OF PHYSICS: CONDENSED MATTER

J. Phys.: Condens. Matter **19** (2007) 315221 (21pp) doi:10.1088/0953-8984/19/31/315221

# A review of the electronic and magnetic properties of tetrahedrally bonded half-metallic ferromagnets

**Ph Mavropoulos**[1] **and I Galanakis**[2]

[1] Institut für Festkörperforschung, Forschungszentrum Jülich, D-52425 Jülich, Germany
[2] Department of Materials Science, School of Natural Sciences, University of Patras, Patras 265 04, Greece

E-mail: ph.mavropoulos@fz-juelich.de and galanakis@upatras.gr

Received 1 November 2006
Published 3 July 2007
Online at stacks.iop.org/JPhysCM/19/315221

**Abstract**

The emergence of the field of spintronics has brought half-metallic ferromagnets to the centre of scientific research. A lot of interest was focused on newly created transition-metal pnictides (such as CrAs) and chalcogenides (such as CrTe) in the metastable zinc-blende lattice structure. These compounds were found to have the advantage of high Curie temperatures in addition to their structural similarity to semiconductors. Significant theoretical activity has been devoted to the study of the electronic and magnetic properties of these compounds in an effort to achieve a better control of their experimental behaviour in realistic applications. This paper is devoted to an overview of the studies of these compounds, with emphasis on theoretical results, covering their bulk properties (electronic structure, magnetism, stability of the zinc-blende phase, stability of ferromagnetism) as well as low-dimensional structures (surfaces, interfaces, nanodots and transition-metal delta-doped semiconductors) and phenomena that can possibly destroy the half-metallic property, like structural distortions or defects.

## Contents

## 1. Introduction

The rapid advance of magnetoelectronics and spintronics in recent years has given a strong boost to the search for novel magnetic materials, such as the half-metallic ferromagnets. These are spin-polarized materials, which exhibit the property of having a metallic density of electron states for the one spin direction (usually majority spin), while there is a band gap around the Fermi level, $E_F$, for states of the opposite spin. This *half-metallic* property (the name coined by de Groot and collaborators [1]) makes the one spin channel conducting, while the other is insulating (or semiconducting), so that, in the ideal case, half-metals can conduct a current which is 100% spin-polarized.

The spin polarization $P$ at $E_F$ is expressed in terms of the spin-up and spin-down density of states, $n_\uparrow(E_F)$ and $n_\downarrow(E_F)$, as

$$P = \frac{n_\uparrow(E_F) - n_\downarrow(E_F)}{n_\uparrow(E_F) + n_\downarrow(E_F)}. \tag{1}$$

For an ideal half-metallic ferromagnet, $P = 1$; however, a number of factors can reduce $P$ to lower values: defects and disorder, spin–orbit coupling, temperature, interface and surface states in the gap, etc. Apart from a polarization value as close as possible to unity, half-metals must have also other properties in order to be functional: a high Curie point $T_C$ and compatibility with semiconductors are among the key points for spintronics applications.

In 2000, Akinaga and collaborators [2] reported growth of a few layers of CrAs in the metastable zinc-blende (zb) phase for the first time; this was achieved by molecular beam epitaxy on a GaAs substrate (the ground state structure of CrAs is the MnP structure [3]). In the zb phase, CrAs was reported to be ferromagnetic, with a Curie point higher than 400 K. In the same publication, first-principles calculations of bulk zb-CrAs showed the material to be a half-metallic ferromagnet; the moment per formula unit was calculated to be 3 $\mu_B$, in agreement with the experimental result.

These findings initiated much activity, because several advantages were combined: the half-metallic property, coherent growth on a semiconductor, and $T_C$ higher than room temperature. The activity was extended beyond zb-CrAs to encompass a variety of tetrahedrally bonded transition-metal (TM) compounds with sp atoms of groups IV, V and VI of the periodic table. In this paper we review relevant investigations to date, with emphasis on theoretical

results on the electronic structure and magnetic properties of these compounds. We do not extend our review to the related but vast topics of diluted magnetic semiconductors or other types of half-metals. We also note in passing the surprising (calculated) appearance of half-metallic ferromagnetism in tetrahedrally bonded compounds of I–V and II–V elements [4–6], such as zb-CaAs, where no transition metals are involved. The origin of ferromagnetism is therefore of a different nature here, but a discussion of these compounds is beyond the purpose of the present work.

The remainder of the paper is summarized as follows. We begin with a summary of experimental findings in section 2. Section 3 is devoted to an analysis of the electronic and magnetic structure of half-metallic zb compounds, as obtained by first-principles calculations. Investigations on the magnetic ground state (ferromagnetic versus antiferromagnetic), exchange interactions and Curie temperatures of such compounds are reviewed in section 4. The metastability of the zb phase, compared to the NiAs or other phases, is addressed in section 5. The possibility of surface half-metallicity is discussed in section 6. In section 7 we review the properties of the interfaces with semiconductors, including delta-doping and transport in multilayered structures. We continue with a discussion on the effect of disorder on the half-metallic gap in section 8. Section 9 is devoted to tetrahedrally bonded TM sp compounds with other structures, such as the wurtzite structure. Finally, in section 10, we review the results of calculations beyond density-functional theory. We conclude with a summary in section 11.

## 2. Experimental results

Experimentally, CrAs in the zb structure was first grown by Akinaga *et al* [2], by molecular beam epitaxy (MBE) on a GaAs substrate. The zb phase could only be stabilized for thin CrAs layers; for samples above a critical thickness of 3 nm, the reflection high-energy electron diffraction (RHEED) pattern indicated an unknown different phase; such small thicknesses are typical in all experiments involving zb pnictides (compounds including group-V atoms) or chalcogenides (compounds including group-VI atoms). The measured saturation magnetization at low temperature corresponded to 3 $\mu_B$ per formula unit, in good agreement with *ab initio* calculations (which also predicted a half-metallic band structure). The precise Curie temperature was not reported, but it was found to be higher than 400 K, suggesting applicability at room temperature. The surface morphology and magnetic characteristics of zb-CrAs films under different growth conditions were studied in [7]. In [8], a thickness-dependence angular resolved photoemission spectroscopy (ARPES) study showed a dispersion for a 2 nm CrAs film which was not present for a 30 nm film; this, together with the RHEED pattern, suggested a monocrystalline sample at 2 nm, changing to polycrystalline one at 30 nm. ARPES data on a thin zb-CrAs film were also presented in [10].

Further work [11], based on fluorescence extended x-ray absorption fine structure (EXAFS), provided more evidence on the existence of the zb phase on a 2 nm zb-CrAs film, and found a CrAs bond length of 2.49 Å (in close agreement with the value of 2.52 Å which is deduced from *ab initio* calculations [12]). Moreover, high-resolution transmission electron microscopy (HRTEM) and x-ray grazing incidence diffraction (GID) were used in [13] to identify 2.5 nm (9 monolayers (ML)) thick zb-CrAs on GaAs; it was found that the zb phase can be partly deformed by appropriate annealing. The samples were ferromagnetic, the saturation magnetic moment of both phases was found to be about 3 $\mu_B$ per formula unit, and $T_C$ was above 400 K.

In parallel, zb-CrAs/GaAs multilayers were grown by use of MBE and studied in [9] and [14]. In both studies the optimal (for the zb structure) multilayers consisted of a period of 2 ML of GaAs and 2 ML of CrAs. The period was repeated 20 times in [9] and 100 times

in [14]. Magnetization measurements in [14] showed a magnetic moment of 2 $\mu_B$ per formula unit of CrAs (lower than the theoretical prediction of 3 $\mu_B$), and a Curie temperature of 800 K.

CrSb was also grown by MBE in ultrathin films of a few monolayers in the zb structure [15, 16]. In the work of [15], GaAs, GaSb and (Al, Ga)Sb substrates were used. The structure was examined by HRTEM and RHEED. The samples were ferromagnetic with a magnetic moment per formula unit reported to be between 3 and 5 $\mu_B$ (the theoretical prediction is 3 $\mu_B$ [17–19]) and a $T_C$ definitely exceeding 400 K. In [16] it was shown how the substrate can be tailored for growth of somewhat thicker films of CrSb. While the maximal thickness on GaAs was found to be 1 nm (3 ML), an (In, Ga)As substrate provides a larger lattice parameter which can be tuned by changing the In composition to favour the growth of zb-CrSb. On an $In_{0.08}Ga_{0.92}As$ substrate, 6 ML of zb-CrSb were successfully grown, and for an $In_{0.13}Ga_{0.87}As$ substrate, growth of a 9 ML (3 nm) zb-CrSb film could be achieved.

Also CrSb/GaAs multilayers were grown in the zb structure [20]. Here, the CrSb thickness was just 1 ML, while the GaAs layers were 5 nm thick, and the multilayers included up to four periods. The zb structure was monitored by RHEED measurements during growth, and cross-checked for dislocations at the interfaces by HRTEM. The saturation magnetization at low temperatures was close to the theoretical value of 3 $\mu_B$. The ferromagnetic transition temperature was reported to be above 400 K (measurements at high temperatures were limited by the superconducting quantum interference device (SQUID)).

MnAs could be grown in nanodots in the zb structure [10, 21, 22][3]. References [10] and [21] report the growth of zb-MnAs dots of average size of about 16 nm on sulfur-terminated GaAs(001) surfaces, with a density of dots of $2.3 \times 10^{10}$ cm$^{-2}$. When the growth was continued, the MnAs dots changed to the NiAs structure (which is the equilibrium structure of MnAs). SQUID measurements showed the zb-MnAs dots to be ferromagnetic, with a Curie temperature of about 280 K. Photoemission spectra [10, 21] show a localization of the Mn d states, with the absence of a Fermi edge[4], a main peak at around 4 eV below $E_F$, and a satellite at 6 eV below $E_F$; these features are similar to (Ga, Mn)As diluted magnetic semiconductors, and quite different from MnAs in the NiAs structure, where a Fermi edge is clearly seen in photoemission [10, 21]. The conclusions of [10] are similar, where it is reported that, with increasing dot density (above $3 \times 10^{12}$ cm$^{-2}$), a Fermi edge evolves in the photoemission spectrum. This onset of metallic behaviour is attributed by the authors either to formation of a NiAs-type of structure or to percolation among the clusters. We also note the possibility of delta-doped GaAs with Mn [23, 24]; see section 7.1 for further discussion.

Further experimental work on zb pnictides and chalcogenides includes MBE growth of GaSb(25 Å)/MnSb(2 Å) (001) multilayers [25] and CrTe on GaAs(001) thin films [26]. In both cases it is reported that there are strong indications of a zb phase, but no definite proof.

Finally, we note that, to our knowledge, the half-metallic property itself has not been experimentally proven or disproven in these compounds.

## 3. Calculations on TM-based zinc-blende compounds

### *3.1. Band structure and density of states*

The principal mechanism leading to the appearance of the half-metallic gap in zb compounds of transition metals (TM) with sp elements is the hybridization of the d wavefunctions of

[3] In [10] it is reported that MnSb dots could not be directly grown in the zb phase on GaAs, probably due to lattice mismatch.

[4] This absence of a Fermi edge, indicating an insulating phase, is not found by *ab initio* calculations. In [10, 21] it is speculated that the reason is strong electron correlations, which are not well captured by local density-functional theory.

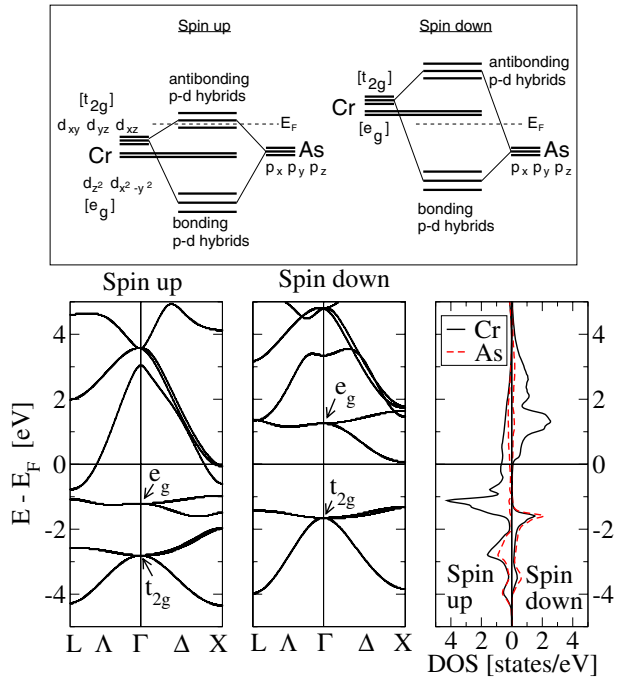


**Figure 1.** Top: schematic description of the p–d hybridization leading to the half-metallic property. Bottom: calculated spin-resolved band structure and spin- and atom-resolved density of states of zb-CrAs in the GaAs lattice parameter within the LSDA.

(This figure is in colour only in the electronic version)

the TM with the p wavefunctions of the sp atom. This p–d *hybridization* is dictated by the tetrahedral environment, where each atom is surrounded by four atoms of the other species. In particular, in the presence of tetrahedral symmetry the d states split in two irreducible subspaces: the threefold-degenerate $t_{2g}$ subspace, consisting of $d_{xy}$, $d_{yz}$ and $d_{xz}$ states, and the twofold-degenerate $e_g$ subspace, which includes the $d_{x^2-y^2}$ and $d_{z^2}$ states. Only states of the former subspace can hybridize with the p states of the sp atom neighbours, forming bonding and antibonding hybrids; the $e_g$ states, on the contrary, remain rather non-bonding. The situation is shown schematically in figure 1 (up) for both spins, with the majority (spin-up) d states being lower in energy than the spin-down states due to the exchange splitting.

Starting from this picture, we can now proceed to a discussion of the energy bands, shown in figure 1 (down), and calculated within the local spin density approximation (LSDA) of density-functional theory (the As 4s states are much lower in energy and are omitted in the figure). We note that the notations $e_g$ and $t_{2g}$ are, strictly speaking, valid only for states at the centre of the Brillouin zone; however, the energy bands formed by the $e_g$ and $t_{2g}$ states are energetically rather separated, therefore we keep this notation for the bands formed by these states. The strong p–d hybridization leads to wide corresponding $t_{2g}$ energy bands, located, for spin-up, at about $-5$ to $-2$ eV (bonding states), at and above $E_F$ (antibonding); the latter are in the same energy range as the Cr s states. The rather non-bonding $e_g$ states, on the contrary, form mainly narrow bands. These remain energetically between the bonding and antibonding p–d bands, at about $-1$ eV. For spin-down, the situation is similar, with all bands shifted to higher energies because of the exchange splitting; the spin-down bands are also wider, because

they reside at higher energies. The striking effect is that, for spin-down, the exchange splitting is strong enough to push the $e_g$ states just above the Fermi level, so that $E_F$ is in the gap. This is also seen in the atom- and spin-resolved density of states (DOS). According to the calculated DOS, the material is manifestly half-metallic in its electronic and magnetic ground state.

This basic form of the electronic DOS is found by all relevant electronic structure calculations, within either the LSDA or the generalized gradient approximation (GGA) to density-functional theory. Calculations within the GGA show a slightly stronger local magnetic moment at the Cr site, resulting in a stronger exchange splitting and a wider gap; then, $E_F$ is even deeper within the gap. It is generally expected that the GGA yields a more accurate prediction of the lattice parameter and magnetic moment in magnetic compounds, with corrections of the order of 2–3%.

The p–d hybridization, essential to the formation of the gap, is well-known as p–d *repulsion* in the physics of TM defects in semiconductors of zb (where the TM substitutes the cation) or diamond structure [27], and is essentially present also in diluted magnetic semiconductors (DMS) [28]. In this respect, the electronic structure of zb pnictides and chalcogenides can be viewed as the electronic structure of TM-doped semiconductors in the limit of high concentration. From the point of view of electronic structure, it is expected that all zb binary compounds of TM with group IV, V, and VI sp atoms are candidates for the appearance of half-metallic ferromagnetism—in fact, their calculated DOS is similar to that of CrAs (e.g. see [2, 19, 29–39]), with spin-down gaps around 0.5–1 eV when the sp element belongs to group IV, around 1–2 eV when it belongs to the group V, and 1.5–2.5 eV when it belongs to the group VI, and with the spin-up bands appropriately shifted to achieve charge neutrality.

The half-metallic state is, however, not guaranteed in all of these compounds, nor is a ferromagnetic ground state. We discuss this in sections 4 and 5. As we shall see, other factors (lattice constant, antiferromagnetic interactions, structural instabilities, etc) limit this expectation, but a number of compounds remain within these limits.

### *3.2. Magnetic moments*

In the bulk of half-metallic compounds, the spin moment per formula unit is an integer (in $\mu_B$). Since $E_F$ is in the gap, the total number of spin-down valence electrons per formula unit, $N_{tot}^{\downarrow}$, is an integer. The total number of valence electrons per formula unit, $Z_{tot}$, must also be an integer, so it follows that the number of valence spin-up electrons, $N_{tot}^{\uparrow} = Z_{tot} - N_{tot}^{\downarrow}$, is an integer. Thus the magnetic moment, $M = (N_{tot}^{\uparrow} - N_{tot}^{\downarrow})\mu_B = (Z_{tot} - 2N_{tot}^{\downarrow})\,\mu_B$, is an integer. This is a necessary, but not sufficient, condition for half-metallicity. (At surfaces or interfaces this can change; see sections 6 and 7.)

Due to the similarity in the DOS of all zb pnictides and chalcogenides, the number of spin-down valence states up to the gap is always four: there is the low-lying s band of the sp atom, and the three bonding p–d ($t_{2g}$) bands. Therefore, assuming half-metallic behaviour, the total moment per formula unit follows a Slater–Pauling-like 'rule of eight':

$$M_{tot} = (Z_{tot} - 8)\,\mu_B. \tag{2}$$

Analogous relations hold for the half-metallic Heusler alloys, where there is a Slater–Pauling rule of 18 (in half-Heusler alloys) and rule of 24 (in full-Heusler alloys) [40]. Thus, in the half-metallic state, CrAs and CrSb have a moment of 3 $\mu_B$, while CrSe or MnAs (having one more valence electron) show a moment of 4 $\mu_B$. Once more an analogy to the diluted magnetic semiconductors can be seen: calculations show that, for instance in $Ga_{1-x}Mn_xAs$, the spin

**Table 1.** Top: local moments (in $\mu_B$) of the TM and sp atoms in zb pnictides and chalcogenides calculated within the LSDA in the (large) InAs lattice parameter (after [19]), showing trends due to electronegativity of the anion. Bottom: effect of changing the lattice parameter on the local magnetic moments of CrAs. The magnetization of the interstitial region (amounting to about half of the volume in the zb structure) is small and not included in the table.

| Compound | CrN | CrP | CrAs | CrSb | MnAs | CrS | CrSe | CrTe |
|---|---|---|---|---|---|---|---|---|
| $M$(TM) | 3.89 | 3.32 | 3.27 | 3.15 | 4.07 | 3.86 | 3.83 | 3.75 |
| $M$(sp) | −1.07 | −0.45 | −0.38 | −0.25 | −0.25 | −0.12 | −0.10 | −0.06 |
| $a_{\text{latt}}$ (Å) | 5.45 | 5.65 | 5.87 | 6.06 | 6.48 | | | |
| $M$ (Cr) ($\mu_B$) | 2.59 | 3.02 | 3.15 | 3.27 | 3.55 | | | |
| $M$ (As) ($\mu_B$) | −0.13 | −0.20 | −0.29 | −0.38 | −0.60 | | | |

moment per Mn atom is exactly 4 $\mu_B$. Note that ternary compounds, such as (Cr, Mn)As, also follow the same rules, as long as all TMs (here Cr and Mn) occupy the same sublattice of the zb structure; for instance, see [41] for calculations on half-metallic CrAs/MnAs(001) superlattices.

From an alternative viewpoint, we can say that the p states, low-lying as they are in energy, act as reservoirs, hosting electrons which are donated by the TM until the p states are filled up with six electrons. The remaining TM d electrons build up the spin moment. This viewpoint neglects the essential p–d hybridization, but is useful for electron counting.

Similar to the pnictides and chalcogenides is the electronic structure of zb-TM compounds with Si, Ge and Sn [31, 42–44]. However, zb-TM compounds with C (e.g. MnC) have a distinctly different density of states, with the half-metallic gap being among the spin-up states, while the spin-down bands are metallic [45, 46]. This gives rise to a 'rule of 12' instead of equation (2), and originates from the huge gap induced by carbon [34].

### *3.3. Local moment trends with cation valence and electronegativity*

In terms of the p–d hybridization one can understand the trends in DOS and local magnetic moment with changing cation valence and/or electronegativity. Firstly we note that the sp atom has a moment oppositely oriented to the one of the TM; calculated values are shown in table 1 (up). To understand this, we observe that the spin-up d states of the TM are lower in energy than the spin-down d states; thus, when p–d hybridization occurs, the bonding spin-up $t_{2g}$ hybrids have a larger d admixture and are more itinerant than the spin-down ones; the latter are more localized within the sp atom. Thus, in the Wigner–Seitz cell of the sp atom, the spin-down states are in the majority, leading to this 'antiferromagnetic' coupling.

According to this picture, the following trends can be deduced under an unchanged lattice parameter. On changing the sp atom for a lighter one of the same group (therefore more electronegative), the p states are shifted to lower energies and the spin-down p–d hybridization is reduced; the spin-down bonding p–d bands become more localized at the sp atom, transferring to its vicinity spin-down charge from the TM. On the other hand, because of the proximity of the spin-up d states, the spin-up hybridization is reduced to a lesser extent (this can be seen by a tight-binding argument, as the hopping decreases with the energy separation). As a result, the local moment of the sp atom increases; the same is true for the local moment of the TM, since the sum, $M_{\text{tot}}$, must be a constant integer. Also the gap increases for lighter sp atoms, because the p states (forming the valence band) are shifted lower, and the $e_g$ states (forming the conduction band) are shifted higher by the stronger local TM moment

and exchange splitting[5]. Note also that TM group-VI compounds show a wider gap than TM group-V compounds, because the p states of the former are lower in energy.

Competing with these effects is the strong reduction in the lattice parameter due to the smaller volume of lighter sp elements. This results in reduction of the local moments (due to stronger hybridization), and also loss of half-metallicity (as we discuss below); in table 1 (down) we show the effect of lattice compression on the local moments of CrAs. As it turns out, the effects of the change of lattice parameter by far outweigh the effects of electronegativity.

### *3.4. Effect of the lattice parameter on half-metallicity*

We now turn to the effect of the lattice parameter on the half-metallic property. We begin by the observation that compression of the lattice shifts all energy levels higher, but has a greater effect on the extended p states (and p–d hybrids), and a lesser effect on the localized $e_g$ states. Since $E_F$ is situated among the spin-up antibonding $t_{2g}$ bands, under lattice compression $E_F$ will be carried to higher energies along with these levels; the position of the spin-down conduction band (which is of $e_g$ character) is less affected by compression. Therefore $E_F$ ultimately enters the $e_g$ conduction band and half-metallicity is lost. It also turns out that, under lattice expansion, $E_F$ enters the spin-down valence band, also causing loss of half-metallicity.

As a conclusion, zb chalcogenides and pnictides are half-metallic in a limited range of lattice parameters, and it is not guaranteed that the equilibrium lattice parameter $a_{eq}$ is in this range. First-principles calculations are needed in order to predict $a_{eq}$ and the magnetic state and DOS at $a_{eq}$. For practical purposes, a deviation from the calculated $a_{eq}$ by a few per cent is acceptable, allowing for a small error in the estimation of $a_{eq}$ by density-functional calculations[6], and for a slightly different lattice parameter of the substrate, on which the compound can grow pseudomorphically. We remind the reader that chalcogenides and pnictides are not at equilibrium in the zb structure, thus they can be grown only for a few monolayers on suitable substrates.

In table 2 we summarize the results of LSDA calculations [19] of the half-metallic property at the lattice parameters of several semiconductors, together with the equilibrium lattice parameter, for several systems. Systems marked with a '+' are half-metallic, with a '−' are not half-metallic, while a '±' means that the system is at the edge of half-metallicity, with $E_F$ just touching the conduction band. Allowing for an LSDA underestimation of the lattice parameter, together with a small lattice mismatch with the semiconductor, we identify which systems can, in principle, be coherently grown (only for a few monolayers; see section 5) on which semiconductors, being at the same time half-metallic; we mark them with a box. In this way, we identify the following candidate combinations: VAs on GaAs, VSb on InAs and GaSb, CrAs on GaAs, CrSb on InAs and GaSb, MnSb on GaSb, VTe on ZnTe, CrSe on ZnSe and CdS, and CrTe on CdSe and ZnTe. Note that nitrides, phosphides and sulfides have very small lattice parameters and are not half-metallic; they are excluded from the table. Mn group-VI compounds are not ferromagnetic, and are also excluded.

### *3.5. Effect of spin–orbit coupling on the polarization*

Spin–orbit coupling introduces a mixing of the two spin channels, so that the electron spin is not a good quantum number. Therefore, if it is present, it is expected that states which were

[5] The exchange splitting is roughly $\sim I \cdot M$, where $M$ is the magnetic moment and $I$ is the exchange integral, having a value of about 0.9 eV $\mu_B^{-1}$ for transition metals.

[6] In particular the LSDA is known in general to underestimate $a_{eq}$ by 2–3%; GGA corrects this to a great extent, but in some systems it can slightly overestimate $a_{eq}$.

**Table 2.** Half-metallic property of several zb pnictides and chalcogenides at the experimental lattice parameters of several semiconductors. The calculated (LSDA) equilibrium lattice parameters are given in parentheses. Systems marked with a '+' are half-metallic, with a '−' are not half-metallic, while a '±' means that the system is at the edge of half-metallicity. A box indicates that a half-metallic system has a suitable lattice parameter to grow on the corresponding semiconductor.

| $a$ (Å) | GaN | InN | GaP | GaAs | InP | InAs | GaSb | InSb |
|---|---|---|---|---|---|---|---|---|
| Compound | 4.51 | 4.98 | 5.45 | 5.65 | 5.87 | 6.06 | 6.10 | 6.48 |
| (5.54) VAs | − | − | − | **+** | + | + | + | + |
| (5.98) VSb | − | − | − | − | + | **+** | **+** | + |
| (5.52) CrAs | − | − | − | **+** | + | + | + | + |
| (5.92) CrSb | − | − | − | − | + | **+** | **+** | + |
| (5.36) MnAs | − | − | − | − | + | + | + | + |
| (5.88) MnSb | − | − | − | − | − | − | **±** | + |
| $a$ (Å) | ZnS | ZnSe | CdS | CdSe | ZnTe | CdTe | | |
| Compound | 5.41 | 5.67 | 5.82 | 6.05 | 6.10 | 6.49 | | |
| (5.56) VSe | − | − | − | + | + | + | | |
| (6.06) VTe | − | − | − | − | **±** | + | | |
| (5.61) CrSe | − | **±** | **+** | + | + | + | | |
| (6.07) CrTe | − | − | − | **+** | **+** | + | | |

previously accounted as spin-up states in the region of the half-metallic gap will now have some contribution to the spin-down DOS; strictly speaking, the half-metallic property ($P = 100\%$) can never be achieved, since some amount of spin–orbit coupling is present in all materials. Then, the half-metallic gap turns into a pseudo-gap, with some spectral intensity.

However, first-principles calculations [47, 48] show that the effect can be small, of the order of 1%, except in the case when heavy elements are present. Thus, when spin–orbit coupling is included in the calculations, CrAs shows a polarization of $P = 99.6\%$, CrSb shows $P = 98.6\%$ (note that Sb is heavier than As) and MnBi shows a much reduced polarization of $P = 77\%$ (neglecting spin–orbit coupling, MnBi is predicted [32, 49] to be half-metallic). These results demonstrate that spin–orbit coupling is significant for a heavy element such as Bi, also because of its 6p states which are directly involved in the band structure around $E_F$. The calculated orbital moment of MnBi is large, too, reaching a value of 0.11 $\mu_B$.

A theoretical analysis based on perturbation theory [47] shows that the spectral properties in the half-metallic spin-down pseudo-gap depend (i) on the spin-up DOS in the same region and (ii) on the proximity of the energy to the band edges. It is deduced (and verified by *ab initio* calculations) that (i) the spin-down DOS is a weak reflection of the spin-up DOS, depending quadratically on the spin–orbit coupling spin-flip strength, $n_\downarrow(E) \sim |V_{so}|^2 n_\uparrow(E)$, and (ii) that, close to the band edges, $n_\downarrow(E)$ increases strongly, so that it must be treated beyond first order in perturbation theory (because of the degeneracy of unperturbed spin-up and spin-down eigenvalues at the band edge).

## 4. Magnetic ground state, exchange interactions and Curie temperature

In the discussion up to now we assumed a ferromagnetic ground state, and experiment has shown that CrAs, CrSb and MnAs in the zb phase are ferromagnetic (see section 2). However, the ferromagnetic ground state has to be attested by calculations for the not-yet-fabricated

compounds. In a number of papers [12, 27, 31, 33, 37, 42, 50–56] this aspect is examined via first-principles calculations. In the framework of such calculations there are three ways to attest the ferromagnetic ground state. (i) Non-collinear magnetic calculations can be made, where the system is allowed to relax in any arbitrary non-collinear configuration. (ii) Total energy calculations can be made in the ferromagnetic and in several antiferromagnetic states (perhaps including disordered local moment states within the coherent potential approximation), seeking the energy minimum. (iii) Starting from a ferromagnetic state, the interatomic exchange constants can be calculated (usually assuming interactions within a Heisenberg model), from which conclusions can be drawn regarding the ground state as well as excited state properties, including the Curie temperature (see section 4.2). These methods are to a great extent complementary, and their applicability depends on the size of the system as well as the computational method used. The most accurate way of calculation is probably (i), but it is often not practical because it requires the use of large supercells, solution of equations coupling the two spin channels, and must be applied to many starting configurations, especially if there are more than one local energy minimum. Thus, (ii) and (iii) are most common in practice, and can in most cases ascertain if the ground state is indeed ferromagnetic or not. We note, however, that if the magnetic ground state is not ferromagnetic, it is likely to be non-collinear, since the fcc geometry (corresponding to the TM sublattice) causes magnetic frustration in the case of antiferromagnetic exchange interactions.

As a general principle (but with notable exceptions, depending mainly on the lattice parameter), the magnetic ground state of TM pnictides and chalcogenides in the zb structure is ferromagnetic, if the total number of valence electrons $Z_{\rm tot} \leqslant 12$. According to equation (2), this means that the maximum moment in the half-metallic state is 4 $\mu_{\rm B}$. Thus, for instance, MnAs is expected to be ferromagnetic, but MnSe or FeAs are expected to be antiferromagnetic (or non-collinear). The reasoning behind this rule is the following. Ferromagnetic order in these compounds is brought about by the double exchange mechanism (energy is gained by a band-broadening at $E_{\rm F}$ due to hybridizations) involving the spin-up antibonding $t_{2g}$ states. Once $Z_{\rm tot}$ exceeds 12, the spin-up $t_{2g}$ states are fully occupied, and the double exchange mechanism is no longer present (the band broadening does not bring any gain in energy); thus the ferromagnetic order is lost[7].

### *4.1. Total energy results*

In accordance with the above, total energy calculations [12] have shown that VAs, CrAs and MnAs are ferromagnetic, while FeAs was found to have an antiferromagnetic ground state (the possibility of a non-collinear state was not examined in [12]). The energy gain for the formation of the ferromagnetic state (compared to the antiferromagnetic) is about 0.2 eV for VAs, 0.3 eV for CrAs and 0.1 eV for MnAs; the antiferromagnetic state of FeAs provides an energy gain of 0.1 eV compared with the ferromagnetic state (all energies calculated within the LSDA) [12]. Calculations on MnTe in the zb structure have shown that it also has an antiferromagnetic ground state [27]. Other calculations have confirmed this aspect. Total energy calculations have confirmed a ferromagnetic ground state for MnAs [50], CrAs [33, 37] and CrSb [33, 37].

A recent study [56] on MnAs concludes that as $E_{\rm F}$ enters the spin-down conduction band there occurs a Fermi surface nesting (i.e. a large area of the spin-down Fermi surface is almost parallel to the spin-up Fermi surface, being separated by an almost constant vector $\vec{q}$), allowing for virtual spin-flip excitations of wavevector $\vec{q}$ and leading to a corresponding non-collinear state. From another viewpoint, it has been suggested [52, 57] that there are two

[7] The same cause of ferromagnetism has been identified in some TM-doped diluted magnetic semiconductors [28], although those systems are rather more complicated involving also a Zener p–d exchange.

factors determining the first-neighbour Mn–Mn interaction in MnAs: a direct Mn(d)–Mn(d) antiferromagnetic interaction and an indirect ferromagnetic Mn(d)–As(p)–Mn(d) interaction. The former is dominant at close Mn–Mn distances, inducing an antiferromagnetic state, but as the lattice parameter increases the overlap of the d states of neighbouring Mn atoms is lost, so that the indirect, ferromagnetic interaction dominates. This fragility of ferromagnetism in MnAs is in accordance with the results of exchange interaction studies (section 4.2).

### *4.2. Exchange interactions in the ground state and calculations of $T_C$*

Sakuma [31] reports a systematic investigation of the interatomic exchange interactions in CrAs, MnSi, MnGe and MnSn in the zb structure. Under the assumption of the validity of a Heisenberg model, with a Hamiltonian of the form

$$H = -\sum_{ij} J_{ij}\,\hat{e}_i\hat{e}_j \tag{3}$$

(where $\hat{e}_i$ is the direction of the magnetic moment at site $i$), the exchange constants $J_{ij}$ are found via the Liechtenstein formula [58]. In this formula, the *ab initio* band structure properties enter, so that the exchange constants are calculated without any adjustable parameter. The coefficient $J_0 = \sum_{i\neq 0} J_{0i}$, corresponding to the band-energy cost for flipping the magnetic moment of a single atom, reflects a 'single-site spin stiffness', and the ferromagnetic state is stable when $J_0 > 0$; a rotation of the local moment by a small angle $\delta\theta$ costs energy $\delta E = J_0(1 - \cos\delta\theta)$, while the mean-field Curie temperature is $T_C^{mf} = 2J_0/3k_B$ (with $k_B$ the Boltzmann constant). This method is not as accurate as a full self-consistent calculation of a magnetic moment flip, but it is much faster and is efficient in showing trends.

All studied compounds in [31] were found to be ferromagnetic for a wide range of lattice parameters; $J_0$ increases as a function of lattice parameter, as $E_F$ enters deeper into the half-metallic gap. Furthermore, by treating $E_F$ as a parameter for a fixed band structure (and calculating $J_0(E_F)$), the relative contribution to the coupling at each energy was found as a function of band-filling. It was shown that the spin-up antibonding $t_{2g}$ states contribute to the ferromagnetic stability, while the spin-down conduction band states ($e_g$ and antibonding $t_{2g}$) induce an antiferromagnetic coupling and cause a change of sign to $J_0$ as $E_F$ enters the conduction band. The highest values for $J_0$ are found for $E_F$ in the middle of the gap. The local-moment-flip energy cost in CrAs, in the GaAs lattice constant (and at the real $E_F$), was found to be about 0.3 eV, which compares well with the ferromagnetic–antiferromagnetic energy difference of 0.3 eV calculated by Shirai [12].

Interatomic exchange interactions were also studied in [37] for V, Cr and Mn compounds with As, Sb and P. It was found that the strongest tendency for ferromagnetism is among the Cr-based compounds, a result verified in [42] for pnictides. In CrAs, the first-neighbour Cr–Cr exchange constant $J_1$ is dominant, of the order of 15 meV. The second-neighbour Cr–Cr interaction $J_2$ is negative (antiferromagnetic) and an order of magnitude smaller (about $-0.1$ meV); due to the half-metallic gap, the exchange constants fall off rapidly with distance.

In [42], the stability of ferromagnetism in zb-CrAs, CrSe, MnAs, MnC, MnSi and MnGe was studied, again based on the calculation of exchange constants. Similarly to [31], lattice compression was found to destabilize the ferromagnetic state, as $E_F$ approaches and enters the spin-down conduction band. The effect was found to be quite drastic in MnAs, with the ferromagnetic Mn–Mn interaction $J_1$ decreasing in magnitude, and the antiferromagnetic Mn–Mn interaction $J_2$ increasing in magnitude; this effect was even stronger in CrSe. (In the other compounds, the trends are similar, but not as drastic.) Thus, as the MnAs lattice parameter is reduced from 5.87 to 5.68 Å (a change of only about 3.5%), the Curie temperature (calculated within the random phase approximation) $T_C^{rpa}$ drops from 551 to 136 K; and CrSe, for a similar

compression, is found to change phase from ferromagnetic to antiferromagnetic ($T_C^{rpa}$ becomes negative). The trend of the mean-field result, $T_C^{mf}$, is similar. An inspection of the DOS leads to the conclusion that the antiferromagnetic susceptibility becomes dominant as $E_F$ enters the spin-down conduction band due to compression; this conclusion is in agreement with the result of Sakuma [31], as well as with the results reported by Kübler [51] and by Sanyal *et al* [56].

Curie temperatures were calculated in [37, 42] and [51]. Several methods have been employed for this purpose. For the solution of the Heisenberg model (after calculation of the exchange constants by Brillouin-zone integration of static-spin-spiral energies), the following have been used: the Monte Carlo method [37] (which is the most accurate), the mean-field approximation (mfa) [37, 42] (overestimating $T_C$), or the random-phase approximation (rpa) [42] (more accurate than the mfa). Alternatively, the approach in [51] identifies the non-local dynamic susceptibility including an adjusted damping parameter. Due to the different approaches in the various works, and without experimental results for $T_C$ in bulk systems, a direct comparison of the result for $T_C$ is meaningless; however, a comparison of $T_C$ trends calculated within the same method is definitely meaningful. It is a common conclusion that the ferromagnetic state is most robust in CrAs, which shows the highest calculated value of $T_C$ (ranging between 790 K and about 1200 K, depending on the method).

## 5. Stability of the zinc-blende phase

The bottleneck for the fabrication of chalcogenides and pnictides in the zb structure seems to be their structural instability. The ground state structure of these compounds is in many cases the hexagonal NiAs structure (MnP structure for CrAs), in which they are not half-metallic. The zb phase is metastable, and needs therefore to be stabilized via pseudomorphic growth on a semiconductor substrate of the zb or diamond structure.

Total energy calculations [18, 34–36, 38, 49, 50, 59–62] have confirmed that the NiAs structure has considerably lower energy than the zb structure for almost all TM pnictides and chalcogenides, with the exception of nitrides [53, 63] which are reported to have a rock-salt ground state (for the early TM compounds ScN–CrN) or a zb ground state (for the late TM compounds, MnN–CoN); the nitrides, however, have too small a lattice parameter to be half metallic, and are beyond the scope of our discussion. The bulk zb phase has typically a higher energy, of the order of $\Delta_{bulk} \sim 0.3$–1 eV per formula unit, than the NiAs phase (when both are calculated at their corresponding equilibrium lattice constants); the NiAs phase also has a considerably smaller equilibrium unit cell volume $V_{eq}$ (e.g. [59] reports for MnAs in the NiAs structure $V_{eq} \approx 31$ Å$^3$ and $V_{eq} \approx 45$ Å$^3$ in the zb structure). It has been reported [35] that $\Delta_{bulk}$ is lower for chalcogenides (CrTe, CrSe and VTe were considered, with $\Delta_{bulk} \sim 0.3$–0.5 eV) than for pnictides ($\Delta_{bulk} \sim 0.5$–1.0 eV), possibly giving an advantage to the growth of chalcogenides in the zb phase.

Typically, under sufficient volume expansion, the NiAs phase becomes unfavourable compared to the zb phase (the energy curves cross, and $\Delta_{bulk}$ becomes negative at some increased lattice constant). However, more important than $\Delta_{bulk}$ is the epitaxial energy difference $\Delta_{epi}$ (i.e. the energy difference between the two phases at a particular lattice constant when a change of the $c/a$ ratio is also allowed), since a compound growing epitaxially on a substrate of increased lattice parameter will be able to adjust its $c/a$ ratio in favour of elastic energy. This was pointed out in [62], where a number of compounds were studied in this aspect (MnAs, CrAs, CrSb, CrS, CrSe and CrTe). It was found that $\Delta_{epi}$ always favours the NiAs phase (for all hypothetical substrate lattice parameters), except for CrSe, for which $\Delta_{epi}$ becomes negative at approximately 6.2 Å, favouring an epitaxial growth in the zb phase for substrates of higher lattice constant. Nevertheless, these conclusions are valid for the growth

of thick layers, while a few monolayers will be much affected by the interfacial energy. This agrees with the experimental observation that CrAs and CrSb can be grown in the zb phase for thicknesses up to a few monolayers, and then break up.

The stability of the zb phase has also been examined with respect to tetragonal and rhombohedral deformation [35, 49, 64–66] (starting from the equilibrium volume in the zb structure). It was found that, under rhombohedral deformation, chalcogenides are stable [35, 65], while, among the studied pnictides, only CrAs, CrSb and MnAs are stable (although rather soft, with shear moduli of the order of 3–5 GPa) [65]. Tetragonal deformation was found to be favourable for MnSb and MnBi [49], with an equilibrium $c/a \sim 0.75$, but the half-metallic character was not changed. This stability of the half-metallic character under tetragonal distortion in many TM pnictides and chalcogenides is the conclusion of a number of works [35, 49, 64, 65, 68, 67]. In particular, a tetragonalization along the [001] direction (expected in the presence of a (001) interface) distinguishes the $z$ axis and causes a splitting of the $t_{2g}$ and $e_g$ irreducible representations at the Brillouin zone centre $\Gamma$ [68]. The $t_{2g}$ threefold degeneracy splits into a twofold degeneracy (involving the $d_{xz}$–$p_y$ and $d_{yz}$–$p_x$ hybrids) and a non-degenerate level (involving the $d_{xy}$–$p_z$ hybrids); the $e_g$ twofold degeneracy splits into two non-degenerate levels, one involving the $d_{z^2}$ levels and one involving the $d_{x^2-y^2}$ levels. These splittings affect the spectral function at $\Gamma$, but they are in no way important for the overall DOS and the gap.

However, in [66] it is reported that a number of compounds (including CrSe and MnAs) cannot be half-metallic even at large substrate lattice constants because of the unfavourable vertical relaxation and $c/a$ ratio. An interesting conclusion of the same work is that, for some pnictides (including CrAs, MnAs and MnSb) the zb phase is unstable with respect to a 'gliding' tetragonal deformation, where the in-plane lattice parameter changes with simultaneous change of the $c/a$ (so that the bond length is kept constant). In practice, however, a tetragonal deformation of this particular kind cannot take place, because the in-plane lattice parameter is fixed by the substrate.

## 6. Surface half-metallicity

The surfaces of half-metallic ferromagnets are not guaranteed to be also half-metallic. This is because wavefunction hybridizations and bonding–antibonding splittings, essential to the appearance of the gap, change significantly at the surface; the 'missing neighbours' can result in the appearance of surface states in the gap, destroying half-metallicity. This is, for instance, the case in most surfaces of half-metallic Heusler alloys [69]. Although half-metallic surfaces are not of particular technological interest (contrary to half-metallic interfaces), they are of value for proving the half-metallic property by spin-polarized photoemission experiments, which are surface sensitive[8]. In zb pnictides and chalcogenides it was demonstrated by *ab initio* calculations [19, 70–72] that the (001) surfaces can, conditionally, be half-metallic.

Surface half-metallicity in the (001) surfaces of these compounds can occur only if they are terminated with the TM. In the case of termination with the sp atom, dangling bonds appear within the half-metallic gap, destroying half-metallicity (the possibility of surface reconstruction was, however, not considered in the calculations in [19, 70]). Similar effects were found in [73].

In case of TM termination, the electronic structure and DOS change at the surface (even if it is half-metallic). A simple electron count shows that, due to the missing sp neighbour, $(8 - Z_{sp})/2$ additional electrons must be accommodated by the surface TM, where $Z_{sp}$ is the

[8] See, e.g., [102] on an experimental study on the (0001) surface of MnSb in the (non-half-metallic) NiAs structure.

valency of the sp atom. To understand this, consider that, in the bulk, these electrons would occupy bonding p–d hybrids; here, half of these hybrids are missing. Local charge neutrality requires that these electrons remain in the vicinity of the surface (mostly in the surface layer). Moreover, half-metallicity is only preserved if they occupy spin-up states (otherwise $E_F$ will enter the conduction band). Therefore, in the cases when half-metallicity is preserved, the spin moment at the surface increases by $(8 - Z_{sp})/2\ \mu_B$ per surface atom. This also leads to an increase of the exchange splitting, shifting the spin-down $e_g$ levels higher in energy, thus also increasing the gap width. Such is the calculated case in, e.g., CrAs, VAs or CrSe. On the other hand, MnAs has a bulk moment of 4 $\mu_B$ per formula unit. If its Mn-terminated, (001) surface were to retain the half-metallic character, the local moment should increase to 5.5 $\mu_B$. This, however, is not possible, since the spin-up $e_g$ and antibonding $t_{2g}$ states can accommodate at most five electrons, leading to a maximum moment of 5 $\mu_B$. As a result, $e_g$ spin-down states are occupied, and half-metallicity is lost.

Also the (110) surfaces of CrP and CrAs were found to be half-metallic in [74, 75] (the calculation of CrP [74] was done at an expanded lattice constant (5.48 Å), at which also bulk half-metallicity appears). Interestingly, the (110) surface contains both kinds of atom (Cr and P or Cr and As), and no dangling bonds appear to destroy the half-metallic property.

Since, from the point of view of electronic structure, all ferromagnetic zb pnictides and chalcogenides are similar, it is expected that surface half-metallicity is likely to appear in such compounds. However, more theoretical investigations are necessary to verify this, examining in particular the effect of lattice relaxations and surface reconstruction.

## 7. Interfaces with semiconductors

For technological applications of half-metals, especially in magnetic tunnel junctions, it is imperative to eliminate the interface states in the gap region (i.e. for spin-down) of the half-metal–semiconductor interface. The reason is that these states can act as carrier reservoirs and contribute to the transport, although they are localized, because the tunnelling rate can be much lower than the refill rate of these states by spin–orbit coupling or inelastic effects [76]. Contacts of half-metallic Heusler alloys with semiconductors are known to host such interface states in almost all studied cases [77]. It is therefore gratifying that pnictides and chalcogenides in the zb structure retain their half-metallicity also at the interfaces with semiconductors (which are anyhow the natural substrate for growth of these half-metals). The reason is that the bonding character changes coherently at the interface. For example, at a CrAs/GaAs interface (with an As interface layer), the p states of the As interface atoms hybridize with the Cr d states on the one side and with the Ga s states on the other. Thus, the bonding–antibonding splitting does not cease at the interface. Such a behaviour is expected also in view of half-metallicity in TM-doped diluted magnetic semiconductors [28].

Interfaces of half-metallic pnictides and chalcogenides in the zb structure with III–V and II–VI semiconductors (in the same structure) were studied theoretically in [68, 73, 78–83]. It was found that no interface states appear at $E_F$ within the half-metallic gap, because of the coherent bonding described above. Moreover, moderate tetragonalization (which is expected in the case of a slight lattice mismatch) was not found to alter the half-metallic character. (See section 5 for a discussion of tetragonalization.)

The half-metallic gap was found to be persistent also in the case of a 50% intermixing at the interfaces [68], in the sense that, at CrAs/GaAs for instance, the interface layer is half occupied by Ga and half by Cr. This is expected, since, again, the bonding continues coherently, and it is known that half-metallicity is present for a wide range of concentrations in diluted magnetic semiconductors such as (Ga, Cr) As [28].

The gap remains present at the interface also in the case that the semiconductor and half-metal anions are different (e.g. CrAs/GaSb). If, however, the valency of the anion changes, the electronic structure is more complicated [68]. As an example we take a CrSb/ZnTe(001) interface, where ZnTe is a II–VI semiconductor, while Sb is a group-V element. Interface states appear at $E_F$ in the case of direct Zn–Sb contact, i.e. if the layered structure is of the form ... CrSbCrSbZnTeZnTe .... On the other hand, if the interface atoms in contact are Cr and Te (structure of the form ... CrSbCrTeZnTe ...), the gap is preserved at the interface. In the latter case, there is also a local increase of magnetic moment at the interface Cr atoms from 3 to 3.5 $\mu_B$ because the Te atoms have one less p hole than the Sb atoms, thus the interface Cr spin-up charge is increased.

### *7.1. Delta-doped zinc-blende semiconductors*

Delta-doping of semiconductors by TM constitutes a special, limiting case of half-metal–semiconductor interface [17, 23, 44, 84]. Such 'digital' compounds are of special interest, because of their two-dimensional half-metallic behaviour and their highly anisotropic transport properties [84]. Also, delta-doping is a possible way to overcome the low solubility limit of TMs in III–V semiconductors, making such constructions interesting as a special case of diluted magnetic semiconductors.

Experiments on GaAs, delta-doped with Mn (in the submonolayer range), found the compound to be ferromagnetic [23]. The Curie temperature dropped with the distance between the Mn delta-layers, but saturated for large distances, indicating ferromagnetism of each single layer. A two-dimensional ferromagnetic, half-metallic character was also found by calculations in GaAs delta-doped with Mn [17, 84]. In [84], the conductivity was also calculated, and it was found that the in-plane conductivity was metallic (only for spin-up), with the current confined at and close to the Mn layers, while the conductivity perpendicular to the plane was extremely low, reflecting the tunnelling between the Mn layers. It is known that ferromagnetic order in DMS (in particular $Ga_{1-x}Mn_xAs$) is assisted by the p holes introduced by the Mn dopants (due to the p–d repulsion) [28]. As Mn-delta-doped GaAs can be viewed as a limiting case of DMS, it is interesting to see [84] that also the p holes are in this case confined at and close to the Mn layers. Calculations on a delta-doped layer of Mn in Si [44] and Ge [85] also showed two-dimensional half-metallic ferromagnetism, based on the same basic mechanism.

In [52], a MnAs/Si superlattice is calculated to induce antiferromagnetic order to MnAs, possibly due to the small lattice parameter; a small 2% tetragonal distortion (with increased $c/a$) restores the ferromagnetic state.

Concerning the exchange interactions, a study of the exchange constants in Mn-delta-doped Ge and GaAs was presented in [86]. It was found that the systems are ferromagnetic, dominated by $J_1 > 0$,[9] while $J_2 < 0$ is lower in magnitude and antiferromagnetic (as is the case in the bulk of zb compounds MnGe and MnAs [42]). Since density-functional calculations underestimate the semiconductor gap, calculations were performed with an ad hoc increased gap, in order to examine its effect on the exchange constants. On increasing the semiconductor gap (either for Ge or for GaAs), the calculations [86] showed the systems to become more 'ferromagnetic', in the sense that $J_1$ increases while $J_2$ decreases in magnitude.

### *7.2. Ab initio interface engineering*

The ferromagnetic and antiferromagnetic properties of TM chalcogenides and pnictides can be applied to novel tunnel junctions. In [76], first-principles calculations showed how one

[9] For the notation see section 4.2.

can design a tunnel junction of half-metallic CrTe elements which are antiferromagnetically coupled via a semiconducting CdTe spacer. The idea is to introduce a monolayer of Mn at the CrTe/CdTe interface, so that the junction is of the form $\ldots(\mathrm{CrTe})_2\mathrm{MnTe}$–$(\mathrm{CdTe})_n$–$\mathrm{MnTe}(\mathrm{CrTe})_2\ldots$ along the [001] direction. Since the Mn–Mn interaction in CdTe is known to be antiferromagnetic, the two magnetic parts of the junction are antiferromagnetically coupled via this interface engineering. The Mn layer also couples antiferromagnetically to the CrTe layers, still resulting in half-metallic parts. The CdTe thickness can be varied so that the interaction energy is tuned to a desirable low level. In the ground state, the junction is insulating, since the spin-up states at $E_\mathrm{F}$ of the two half-metallic parts are in opposite spin directions. Application of an external magnetic field can orient the moments of both half-metallic parts in parallel, so that electrons can tunnel between the spin-up bands of the half-metallic parts, switching on the conductance. Since such a junction is free of interface states at $E_\mathrm{F}$ in the half-metallic gap, its realization would constitute an ideal half-metal–semiconductor switch.

A recent investigation [55] examined CrSe/MnSe and CrTe/MnTe ferromagnetic/antiferromagnetic (001) interfaces. Since MnSe and MnTe are antiferromagnetic semiconductors, while CrSe and CrTe are ferromagnets, an exchange bias is formed at the interface. The antiferromagnetism was reported to be layer-by-layer in the {001} direction. It was found that, in the case of an uncompensated antiferromagnetic (001) interface (where the antiferromagnetic layers are perpendicular to the interface plane), a collinear half-metallic magnetic state is formed throughout the junctions, with an exchange bias of $\Delta E = -0.41\ \mathrm{eV}/a^2$ for CrSe/MnSe and $-0.23\ \mathrm{eV}/a^2$ for CrTe/MnTe (here, $a$ is the in-plane lattice parameter). In the compensated (001) interface (where the antiferromagnetic layers are parallel to the interface plane), a spin-flop (non-collinear) ground state was found, with the Cr moments being perpendicular to the Mn moments; the corresponding exchange bias is $\Delta E = -0.08\ \mathrm{eV}/a^2$ for CrSe/MnSe and $-0.03\ \mathrm{eV}/a^2$ for CrTe/MnTe. A similar spin-flop sate was also calculated in [54] in $(\mathrm{CrSe})_1(\mathrm{MnSe})_1$ and (CrTe)/(MnTe) multilayers. In view of the fragile ferromagnetism [42] and half-metallicity [66] of CrSe, we consider these conclusions rather more important for CrTe/MnTe than for CrSe/MnSe.

## 8. Effect of disorder

The half-metallic property of zb-TM pnictides and chalcogenides is based on the hybridization gap formed by the d states of the TM and the p states of the sp atom, and on the large exchange splitting pushing the spin-down $e_g$ states high in energy. Therefore, disorder (e.g. in the form of antisites or swaps) is expected to result in a loss of half-metallicity, since the p–d hybridization is expected to change at an impurity, and the magnetic moment of an impurity can be lower than the moment of the TM.

The energetics of Cr–As swaps in zb-CrAs have been calculated from first principles in [88] for swaps up to 10%. Three magnetic states were considered for the $\mathrm{Cr_{As}}$ antisites (Cr at the As position): ferromagnetic, antiferromagnetic and spin-glass. It was found that the Cr–As swap is not favoured energetically in any of these cases. However, if such a swap occurs, it was found that the Cr antisites are antiferromagnetically coupled to the rest of the Cr atoms (leading to a ferrimagnetic overall picture), with an energy gain of about 2 eV per Cr antisite compared to the ferromagnetic swap-state; the spin-glass energy was still higher. Furthermore, it was found that the Cr antisites introduce states at $E_\mathrm{F}$ within the half-metallic gap, destroying the half-metallic property.

In another study [80], the mixing energy of As antisites in zb-$(\mathrm{Cr}_{1-x}\mathrm{As}_x)\mathrm{As}$ was calculated, with respect to the phase separated zb-CrAs and pure As. It was found that, if

As is in the ground-state trigonal structure ($\alpha$-As), phase separation is favoured leading to clean zb-CrAs. If, however, As is in the diamond structure (which could be stabilized by a GaAs substrate), the formation of $As_{Cr}$ antisites is favoured for $x \approx 0.6$. In the presence of $As_{Cr}$ antisites, it was found that spin-down states are introduced at $E_F$, and half-metallicity is lost.

Furthermore, the effect of antisites on the DOS and on the magnetic moments was studied in [89] for CrAs, CrSb, CrSe, CrTe, VAs, and MnAs. Alloys of the type $Cr_{1+x}As_{1-x}$, for $-0.5 < x < 0.5$, (and similarly for the other compounds) were calculated. Notably, it was found that half-metallicity is possible in some disordered cases. $Mn_{1+x}As_{1-x}$, for $x > 0$, remained half-metallic, with an increase of the magnetic moment (the $Mn_{As}$ antisites were found to align ferromagnetically to the rest of the Mn atoms). Also in all Cr compounds, for $x > 0$, the half-metallic character is kept (for not-too-high values of $x$), while the magnetic moment dropped (the Cr antisites were found to align antiferromagnetically to the rest of the Cr atoms).

## 9. Other tetrahedrally bonded structures

### *9.1. TM-based wurtzite compounds*

The tetrahedral environment in zb-TM pnictides and chalcogenides is the essential factor for the formation of p–d hybrids and the gap. Therefore, one expects that TM pnictides and chalcogenides in the wurtzite structure (wz), which provides an almost tetrahedral environment, should also be half-metallic. Based on these ideas, Xie *et al* [87] made a systematic theoretical study of such wz compounds, including MnSb, CrAs, CrSb, VAs, VSb, CrSe, CrTe, VSe and VTe. They concluded that half-metallicity should also be present for the wz structure. The DOS is very similar to the one in the zb structure; in the energy bands there is a degeneracy lifting at the Brillouin zone centre, since there is no tetrahedral symmetry (the environment of each atom is almost, but not exactly, tetrahedral). The total moments follow the 'rule of eight' (equation (2)). Half-metallicity in wz CrS, CrSe, CrTe was also reported in [90]. Bismuth-based compounds in the wz structure were studied in [91]. VBi and CrBi were found to be half-metallic at their respective equilibrium lattice parameters (neglecting the strong spin–orbit coupling caused by Bi), while MnBi was found not to be half-metallic; a lattice expansion was needed to restore half-metallicity.

Total energy calculations [61] reveal that the energy of the TM pnictides' wz structure is very close to the energy of the zb structure, and the lattice constants of the two phases are almost equal. This means that the wz structure is also metastable.

### *9.2. Nanoclusters and nanodots*

Nanoclusters of zb-TM pnictides and chalcogenides have also been studied theoretically [92, 93]. This is interesting in view of the experimental results on MnAs nanodots [10, 21, 22], although the calculated nanoclusters are much smaller, not exceeding a size of 50 atoms (the experimental nanodots were 16 nm in diameter). Reference [92] presents results on free-standing nanoclusters $TM_{13}X_{16}$ with TM = (V, Cr, Mn) and X = (N, P, As, Sb, S, Se, Te). By changing the lattice constant, several ferromagnetic and antiferromagnetic magnetic configurations were arrived at (although no total energy results were reported). The sp atoms at the cluster boundary were found to produce dangling bonds, affecting in some cases the half-metallic character. When CrAs nanoclusters were embedded in a GaAs matrix, the dangling bonds were found to vanish, due to the bonding of the boundary

atoms with the matrix. In [93] the focus was in a free-standing zb MnAs nanocluster containing 41 atoms of which 13 were Mn atoms (including a central Mn atom and a first shell of 12 Mn atoms). Structural relaxation was taken into account. It was found that, in the ground state, the central atom couples antiferromagnetically to the first shell. The ferromagnetic state was 125 meV higher, and half-metallic, with a gap of 1.83 eV.

## 10. Recent results on the role of electron correlations and on the temperature dependence of the polarization

Density-functional calculations, within the LSDA or GGA, can capture only a part of the electron exchange and correlation effects. In particular, dynamic effects need to be described by more elaborate (and computationally heavier) extensions, such as the LSDA + DMFT (dynamical mean-field theory).

An interesting effect of dynamic electron correlations on half-metallic ferromagnets is the appearance of non-quasiparticle states (NQS) in the half-metallic gap just above $E_F$. These states, originating from virtual electron–magnon scattering processes, are captured within the DMFT and were calculated in [94] for the case of CrAs. The NQS appear at characteristic magnon energies, i.e. a few tens of meV above $E_F$, and can therefore affect the transport properties even at small voltages. However, to our knowledge, their exact effect on spin-polarized transport has not yet been clarified; such states should be present in all half-metallic systems, because the mechanism that brings them about is rather general [95].

Another effect of dynamic correlations can be a shifting of spectral weight towards the Fermi level, which is expected due to the form of the real part of the self-energy $\Sigma(E)$ near $E_F$: $\mathrm{Re}[\partial\Sigma/\partial E]_{E_F} < 0$.[10] This has an interesting effect on VAs, as was calculated in [96]. Within the LSDA (or GGA), VAs is found to be a ferromagnetic semiconductor, because $E_F$ lies exactly between the spin-up $e_g$ and antibonding $t_{2g}$ states (for spin-down it is in the half-metallic gap). The spin-up gap is tiny, of the order of 50 meV. Within the LSDA+DMFT, it is found that the spin-up $e_g$ and $t_{2g}$ states are shifted towards the Fermi level, closing the gap completely and causing a transition from semiconducting to half-metallic behaviour.

We would also like to point out the problem of absence of a Fermi edge observed in the photoemission spectroscopy of ferromagnetic zb-MnAs nanodots [10, 21] (see also section 2). This is in contrast to theoretical results within density-functional theory, and to our knowledge its explanation is an open problem which deserves more attention in the future.

An open question is the behaviour of the spin polarization $P$ at $E_F$ at elevated temperatures $T$, since it is obvious that $P$ must drop at high $T$. Only few theoretical attempts have been made in this direction [97–100], examining different mechanisms that can contribute to the drop of $P(T)$. These depend on many factors, including the exact band structure and position of $E_F$ in the gap, but the theoretical methods have not been applied to zb pnictides and chalcogenides. In order to obtain a quantitative result, these theories have to be refined and unified (in our opinion, this is one of the most challenging theoretical problems in the field of half-metallic ferromagnets); they indicate, however, that a high $P$ at room temperature requires (i) $T_C$ to be considerably higher than room temperature and (ii) $E_F$ to be deep in the gap, and not in the proximity of a band edge. Experimentally, $P(T)$ can be approached indirectly via transport measurements in magnetic tunnel junctions under some assumptions on the polarization dependence of the magnetoresistance [101].

[10] $\Sigma(E)$ represents a measure of renormalization of the spectral density due to correlations; the Green function, of which the poles determine the spectrum, has the form $G(E) = (E - H^0 - \Sigma(E))^{-1}$, where $H^0$ is the Hamiltonian in the absence of electron correlations.

## 11. Summary and outlook

In this paper we have summarized the work reported on TM pnictides and chalcogenides in the zb structure. Relatively few experimental results have been published. We believe that this is due to the difficulties in experimental growth of these structures. So far, experimental fabrication has been demonstrated only for ultrathin layers (including multilayers) of CrAs and CrSb and nanodots of MnAs, and evidence exists for ultrathin layers of MnAs and CrTe (see section 2). Magnetic measurements have been reported, but no evidence has been shown of half-metallic behaviour (or of its absence, except for the insulating phase reported for zb-MnAs nanodots [10, 21]). At the same time, there are many theoretical and computational investigations on the subject, including other related structures. To a great extent, these concern the structural stability of the zb phase (see section 5), and demonstrate that this phase can be grown epitaxially for a few layers at most (in agreement with experiments on CrAs and CrSb). Although no prediction on future experimental results can be made, we conclude that, if zb pnictides or chalcogenides are to be used in spintronics applications (such as magnetic tunnel junctions or spin injection), it has to be done in such a way that a few monolayers are sufficient.

On the other hand, from the point of view of calculated electronic structure and transport, these compounds are excellent, and growth of a few monolayers is probably enough for applications. Theoretical investigations show that, at the contact with semiconductors, no interface states are present in the gap, and that the half-metallic state is also robust against tetragonal distortions. The ferromagnetic interactions are dominant even in delta-doped (i.e. 1 ML) cases, so that even a single monolayer should be enough to provide fully spin-polarized transport. Calculations including dynamic correlations show that the half-metallic property (at least in CrAs) is not affected, except for the non-quasiparticle states just above $E_F$.

The material with the most robust ferromagnetism is probably CrAs, which is found by calculations to have the highest Curie temperature. It is reasonable to assume that, among the materials which were reviewed here, the best candidates for future applications are CrAs and CrSb (since they are the zb pnictides fabricated so-far), or delta-doped compounds (including Si and Ge) in the monolayer or submonolayer range.

## References


[1] de Groot R A, MÏller F M, van Engen P G and Buschow K H J 1983 *Phys. Rev. Lett.* **50** 2024
[2] Akinaga H, Manago T and Shirai M 2000 *Japan. J. Appl. Phys.* **39** L1118
[3] Watanabe H, Kazama N, Yamaguchi Y and Ohashi M 1969 *J. Appl. Phys.* **40** 1128
Boller H and Kallel A 1971 *Solid State Commun.* **9** 1699
[4] Kusakabe K, Geshi M, Tsukamoto H and Suzuki N 2004 *J. Phys.: Condens. Matter* **16** S5639
[5] Sieberer M, Redinger J, Khmelevskyi S and Mohn P 2006 *Phys. Rev.* B **73** 024404
[6] Yao K L, Jiang J L, Liu Z L and Gao G Y 2006 *Phys. Lett.* A **359** 326
[7] Mizuguchi M, Akinaga H, Manago T, Ono K, Oshima M and Shirai M 2002 *J. Magn. Magn. Mater.* **239** 269
[8] Mizuguchi M, Ono K, Oshima M, Okabayashi J, Akinaga H, Manago T and Shirai M 2002 *Surf. Rev. Lett.* **9** 331
[9] Mizuguchi M, Akinaga H, Manago T, Ono K, Oshima M, Shirai M, Yuri M, Lin H J, Hsieh H H and Chen C T 2002 *J. Appl. Phys.* **91** 7917
[10] Oshima M, Ono K, Mizuguchi M, Yamada M, Okabayashi J, Fujimori A, Akinaga H and Shirai M 2002 *Int. J. Mod. Phys.* B **16** 1681
[11] Ofuchi H, Mizuguchi M, Ono K, Oshima M, Akinaga H and Manago T 2003 *Nucl. Instrum. Methods* B **199** 227
[12] Shirai M 2001 *Physica* E **10** 143
[13] Bi J F, Zhao J H, Deng J J, Zheng Y H, Li S S, Wu X G and Jia Q J 2006 *Appl. Phys. Lett.* **88** 142509
[14] Akinaga H and Mizuguchi M 2004 *J. Phys.: Condens. Matter* **16** S5549
[15] Zhao J H, Matsukura F, Takamura K, Abe E, Chiba D and Ohno H 2001 *Appl. Phys. Lett.* **79** 2776
[16] Deng J J, Zhao J H, Bi J F, Niu Z C, Yang F H, Wu X G and Zheng H Z 2006 *J. Appl. Phys.* **99** 093902

[17] Shirai M, Ogawa T, Kitagawa I and Suzuki N 1998 *J. Magn. Magn. Mater.* **177–181** 1383
[18] Liu B G 2003 *Phys. Rev.* B **67** 172411
[19] Galanakis I and Mavropoulos P 2003 *Phys. Rev.* B **67** 104417
[20] Zhao J H, Matsukura F, Takamura K, Chiba D, Ohno Y, Ohtani K and Ohno H 2003 *Mater. Sci. Semicond. Process.* **6** 507
[21] Ono K, Okabayashi J, Mizuguchi M, Oshima M, Fujimori A and Akinaga H 2002 *J. Appl. Phys.* **91** 8088
[22] Okabayashi J, Mizuguchi M, Ono K, Oshima M, Fujimori A, Kuramochi H and Akinaga H 2004 *Phys. Rev.* B **70** 233305
[23] Kawakami R K, Johnston-Halperin E, Chen L F, Hanson M, Guebels N, Speck J S, Gossard A C and Awschalom D D 2000 *Appl. Phys. Lett.* **77** 2379
[24] Tanaka M 2005 *J. Cryst. Growth* **278** 25
[25] Choi J Y, Choi J Y, Choi S Y, Hong S C and Cho S L 2005 *J. Korean Phys. Soc.* **47** S497
[26] Sreenivasan M G, Hou X J, Teo K L, Jalil M B A, Liew T and Chong T C 2006 *Thin Solid Films* **505** 133
[27] Wei S-H and Zunger A 1987 *Phys. Rev.* B **37** 8958
Wei S-H and Zunger A 1987 *Phys. Rev.* B **35** 2340
[28] Akai H 1998 *Phys. Rev. Lett.* **81** 3002
Sato K, Dederichs P H, Katayama-Yoshida H and Kudrnovský J 2004 *J. Phys.: Condens. Matter* **16** S5491
[29] Zhang M, Hu H, Liu G, Liu Z, Cui Y and Wu G 2004 *J. Low Temp. Phys.* **135** 267
[30] Yao K L, Gao G Y, Liu Z L and Zhu L 2005 *Solid State Commun.* **133** 301
[31] Sakuma A 2002 *J. Phys. Soc. Japan* **71** 2534
[32] Xu Y Q, Liu B G and Pettifor D G 2002 *Phys. Rev.* B **66** 184435
[33] Shirai M 2003 *J. Appl. Phys.* **93** 6844
[34] Pask J E, Yang L H, Fong C Y, Pickett W E and Dag S 2003 *Phys. Rev.* **67** 224420
[35] Xie W H, Xu Y Q, Liu B G and Pettifor D G 2003 *Phys. Rev. Lett.* **91** 037204
Xie W H, Xu Y Q, Liu B G and Pettifor D G 2003 *Phys. Rev. Lett.* **91** 219901 (erratum)
[36] Xie W H and Liu B G 2003 *J. Phys.: Condens. Matter* **15** 5085
[37] Sanyal B, Bergqvist L and Eriksson O 2003 *Phys. Rev.* B **68** 054417
[38] Zhang M, Hu H, Liu G, Cui Y, Liu Z, Wang J, Wu G, Zhang X, Yan L, Liu H, Meng F, Qu J and Li Y 2003 *J. Phys.: Condens. Matter* **15** 5017
[39] Zhang M, Hu H N, Liu Z H, Liu G D, Cui Y T and Wu G H 2004 *J. Magn. Magn. Mater.* **270** 32
[40] Galanakis I, Dederichs P H and Papanikolaou N 2002 *Phys. Rev.* B **66** 134428
Galanakis I, Dederichs P H and Papanikolaou N 2002 *Phys. Rev.* B **66** 174429
[41] Fong C Y, Qian M C, Pask J E, Yang L H and Dag S 2004 *Appl. Phys. Lett.* **84** 239
[42] Sasioglu E, Galanakis I, Sandratskii L M and Bruno P 2005 *J. Phys.: Condens. Matter* **17** 3915
[43] Liu G Q and Liu B G 2006 *Phys. Rev.* B **73** 045209
[44] Qian M C, Fong C Y, Liu K, Pickett W E, Pask J E and Yang L H 2006 *Phys. Rev. Lett.* **96** 027211
[45] Qian M C, Fong C Y and Yang L H 2004 *Phys. Rev.* B **70** 052404
[46] Dag S, Tongay S, Yildirim T, Durgun E, Senger R T, Fong C Y and Ciraci S 2005 *Phys. Rev.* B **72** 155444
[47] Mavropoulos P, Sato K, Zeller R, Dederichs P H, Popescu V and Ebert H 2004 *Phys. Rev.* B **69** 054424
[48] Shirai M, Ikeuchi K, Taguchi H and Akinaga H 2003 *J. Supercond.* **16** 27
[49] Zheng J C and Davenport J W 2004 *Phys. Rev.* B **69** 144415
[50] Zhao Y-J, Geng W T, Freeman A J and Delley B 2002 *Phys. Rev.* B **65** 113202
[51] Kübler J 2003 *Phys. Rev.* B **67** 220403
[52] Kim M and Freeman A J 2004 *Appl. Phys. Lett.* **85** 4983
[53] Miao M S and Lambrecht W R L 2005 *Phys. Rev.* B **71** 214405
[54] Nakamura K, Ito T and Freeman A J 2005 *Phys. Rev.* B **72** 064449
[55] Nakamura K, Kato Y, Akiyama T, Ito T and Freeman A J 2006 *Phys. Rev. Lett.* **96** 047206
[56] Sanyal B, Eriksson O and Aron C 2006 *Phys. Rev.* B **74** 184401
[57] Asada T and Terakura K 1993 *Phys. Rev.* B **47** 15992
[58] Liechtenstein A I, Katsnelson M I, Antropov V P and Gubanov V A 1987 *J. Magn. Magn. Mater.* **67** 65
[59] Sanvito S and Hill N A 2000 *Phys. Rev.* B **62** 15553
[60] Continenza A, Picozzi S, Geng W T and Freeman A J 2001 *Phys. Rev.* B **64** 085204
[61] Miao M S and Lambrecht W R L 2005 *Phys. Rev.* B **71** 064407
[62] Zhao Y J and Zunger A 2005 *Phys. Rev.* B **71** 132403
[63] Lambrecht W R L, Miao M S and Lukashev P 2005 *J. Appl. Phys.* **97** 10D306
[64] Yamana K, Geshi M, Tsukamoto H, Uchida I, Shirai M, Kusakabe K and Suzuki N 2004 *J. Phys.: Condens. Matter* **16** S5815
[65] Shi L J and Liu B G 2005 *J. Phys.: Condens. Matter* **17** 1209

[66] Miao M S and Lambrecht W R L 2005 *Phys. Rev.* B **72** 064409
[67] Miao M S and Lambrecht W R L 2005 *J. Appl. Phys.* **97** 10C304 39 of 138
[68] Mavropoulos P, Galanakis I and Dederichs P H 2004 *J. Phys.: Condens. Matter* **16** 4261
[69] Jenkins S J 2004 *Phys. Rev.* B **70** 245401
Jenkins S J and King D A 2002 *Surf. Sci.* **501** L185
Jenkins S J and King D A 2001 *Surf. Sci.* **494** L793
Ležaić M, Galanakis I, Bihlmayer G and Blügel S 2005 *J. Phys.: Condens. Matter* **17** 3121
Galanakis I 2002 *J. Phys.: Condens. Matter* **14** 6329
[70] Galanakis I 2002 *Phys. Rev.* B **66** 012406
[71] Kang B S, Oh S K, Chung J S and Kang H J 2005 *Thin Solid Films* **488** 204
[72] Byun Y, Lee J I and Jang Y R 2006 *J. Appl. Phys.* **99** 08J101
[73] Qian M C, Fong C Y, Pickett W E, Pask J E, Yang L H and Dag S 2005 *Phys. Rev.* B **71** 012414
[74] Lee J I, Byun Y and Jang Y R 2006 *Surf. Sci.* **600** 1608
[75] Lee J I and Hong S C 2006 *IEEE Trans. Magn.* **42** 2936
[76] Mavropoulos P, Ležaić M and Blugel S 2005 *Phys. Rev.* B **72** 174428
[77] Attema J J, de Wijs G A and de Groot R A 2006 *J. Phys. D: Appl. Phys.* **39** 793
Nagao K, Miura Y and Shirai M 2006 *Phys. Rev.* B **73** 104447
Galanakis G, Ležaić M, Bihlmayer G and Blügel S 2005 *Phys. Rev.* B **71** 214431
Galanakis I 2004 *J. Phys.: Condens. Matter* **16** 8007
[78] Shirai M 2004 *J. Phys.: Condens. Matter* **16** S5525
[79] Nagao K, Shirai M and Miura Y 2004 *J. Appl. Phys.* **95** 6518
[80] Bengone O, Eriksson O, Fransson J, Turek I, Kudrnovsky J and Drchal V 2004 *Phys. Rev.* B **70** 035302
[81] Cha G B, Cho S G and Hong S C 2004 *Phys. Status Solidi* b **241** 1423
[82] Fong C Y and Qian M C 2004 *J. Phys.: Condens. Matter* **16** S5669
[83] Wu R Q, Liu L, Peng G W and Feng Y P 2006 *J. Appl. Phys.* **99** 093703
[84] Sanvito S and Hill N A 2001 *Phys. Rev. Lett.* **87** 267202
[85] Continenza A, Antoniella F and Picozzi S 2004 *Phys. Rev.* B **70** 035310
[86] Picozzi S, Ležaić M and Blügel S 2006 *Phys. Status Solidi* a **203** 2738
[87] Xie W H, Liu B G and Pettifor D G 2003 *Phys. Rev.* B **68** 134407
[88] Shirai M, Seike M, Sato K and Katayama-Yoshida H 2004 *J. Magn. Magn. Mater.* **272–276** 344
[89] Galanakis I, Özdoğan K, Şaşıoğlu E and Aktas B 2006 *Phys. Rev.* B **74** 140408(R)
[90] Zhang M, Bruck E, de Boer F R, Liu G D, Hu H N, Liu Z H, Cui Y T and Wu G C 2004 *J. Mater. Res.* **19** 2738
[91] Zhang M, Bruck E, de Boer F R and Wu G H 2005 *J. Appl. Phys.* **97** 10C306
[92] Nakao M 2004 *Phys. Rev.* B **69** 214429
[93] Qian M C, Fong C Y, Pickett W E and Wang H Y 2004 *J. Appl. Phys.* **95** 7459
[94] Chioncel L, Katsnelson M I, de Wijs G A, de Groot R A and Lichtenstein A I 2005 *Phys. Rev.* B **71** 085111
[95] Irkhin V Y and Katsnelson M I 2002 *Eur. Phys. J.* B **30** 481
[96] Chioncel L, Mavropoulos P, Ležaić M, Blügel S, Arrigoni E, Katsnelson M I and Lichtenstein A I 2006 *Phys. Rev. Lett.* **96** 197203
[97] Itoh H, Ohsawa T and Inoue J 2000 *Phys. Rev. Lett.* **84** 2501
[98] Skomski R and Dowben P A 2002 *Europhys. Lett.* **58** 544
[99] Chioncel L, Arrigoni E, Katsnelson M I and Lichtenstein A I 2006 *Phys. Rev. Lett.* **96** 137203
[100] Ležaić M, Mavropoulos P, Enkovaara J, Bihlmayer G and Blügel S 2006 *Phys. Rev. Lett.* **97** 026404
[101] Garcia V, Bibes M, Barthélémy A, Bowen M, Jacquet E, Contour J-P and Fert A 2004 *Phys. Rev.* B **69** 052403
[102] Rader O, Ležaić M, Blügel S, Fujimori A, Kimura A, Kamakura N, Kakizaki A, Miyanishi S and Akinaga H 2005 *New J. Phys.* **7** 111